Estimation of Surface Tension of Aqueous Polymer Solutions Using Soft Computing Approaches

Esmaili Paeen Afrakoti, Iman; Amooey, Ali Akbar*[+]

Faculty of Technology and Engineering, University of Mazandaran, Babolsar, I.R. IRAN

ABSTRACT: *The surface tension of aqueous polymer solutions is an important property that plays a vital role in mass and heat transfer. In this study, the surface tension of a polymer mixture is modeled using four algorithms (Adaptive Neuro-Fuzzy Inference System (ANFIS), Multi-Layer Perceptron (MLP), Radial Basis Function (RBF), and Adaptive group of Ink Drop Spread (AGIDS)) which has been developed in the soft-computing domain. In this paper, four models for predicting the surface tension are applied and the results were compared with our published experimental data and it was found that the predictions of these models fit the experimental data very accurately. Also, a comparison has been done to evaluate the effectiveness of the relevant four algorithms in the current problem. The simulation results have shown that ANFIS and RBF model predictions are more accurate than the two others in the current problem.*

Keywords: *Soft-computing; Prediction; Surface tension; Polymer solution.*

INTRODUCTION

One of the significant properties of industrial processes is the surface tension of a mixture. It can influence the mass transfer and hydrodynamic rate in multi-phase systems such as extraction, absorption, etc. surface tension aqueous polymer solution. Knowledge of surface tension aqueous polymer solution is required for research on pool boiling of these fluids due to influencing bubble formation in the bulk as well as on the boiling surface [1]. Surface tensions of polymers are significant in the technology of textiles, plastics, coatings, films, and adhesives through their effects on the processes of wetting, adsorption, and adhesion[2, 3].

Interactions between water and soluble polymer in aqueous solution are of great interest from the fundamental standpoint in the process of enhanced oil recovery, processed food, paint, and cosmetics [4-5].

Most high polymers are, however, very viscous even at high temperatures. Furthermore, they exhibit non-Newtonian theology. Considerable care is, therefore, required to ensure valid measurements [2]. Different methods have been applied to obtain mixture surface tension except the aqueous polymer such as activity coefficient model [6], gradient theory [7], and perturbation theory [8]. To date, there are no publications concerning the modeling of surface tension on the aqueous polymer field.

In the past decade, soft computing has been a hot research area because of its ability to reason and learn in an environment of uncertainty and imprecision. Different soft computing algorithms have been used in many engineering fields and have shown their ability to control, model, predict, etc. problems [9–12]. In this research,

** To whom correspondence should be addressed.*
+ E-mail: aliakbar_amooey@yahoo.com
1021-9986/2023/5/1649-1665 18/$/6.08

three types of soft computing algorithms, consisting of fuzzy modeling, artificial neural network, and neuro-fuzzy approaches are being used for modeling of surface tension of the aqueous polymer such as PEG 200 + Water, PEG 300 + Water, PEG 6000 + Water and PPG 2000 +Ethanol. The AGIDS (from fuzzy domain), MLP and RBF (both from artificial neural network approach) and ANFIS (from neuro-fuzzy approach) algorithms, have shown their performance in many applications for solving hard problems [13–15]. In the current research, their ability in the modeling of surface tension of the aqueous polymer problem is investigated and compared to each other.

EXPERIMENTAL SECTION

As mentioned in the previous article [16], Absolute ethanol GR (>99.8%), and poly (ethylene glycol) with average number molecular weights of 200 and 300 (stated purity ≤ 99.0% (mass)) were purchased from Merck. Also, poly (ethylene glycol) with MW=6000 (purity ≤ 99.0% (mass)) and propylene glycol 2000 (purity ≤ 99.0% (mass)) were from Fluka and Riedel-deHaen, respectively. The polymer's polydispersity was equal to 1 and double-distilled water was used in making the solutions. The solutions were prepared in mass, using an analytical balance with ± 0.1mg accuracy. The surface tension measurements were carried out using a thermostated tensiometer (model K9 Kruss Germany) with an accuracy of ± 0.1mN/m, at temperatures of (298.2, 308.2, 313.2, 318.2, 328.2, and 338.2) K and atmospheric pressure.

OVERVIEW OF SOFT-COMPUTING ALGORITHMS

In this section, a brief explanation of different soft-computing algorithms which are used in this paper is given.

ANFIS

Using the advantages of artificial neural network and fuzzy modelling concepts, ANFIS plays a significant role in many real-world applications such as modeling, control, pattern recognition and etc. as a powerful hybrid neuro-fuzzy algorithm in soft-computing domain [17-21].

In Fig. 1, the five layer structure of ANFIS algorithm is shown with a pictorial definition of each layers task. First layer consists of several node, which each node apply a membershipfunction M_{ij} to the corresponding input variable x_i and generates a confidence degree between 0 and 1 as an output of the node.

The output of nodes in layer 2 is computed by application of a T-norm operator such as production to its inputs value which come from layer 1 like $w_1 = M_{11}(x_1) \times M_{21}(x_2)$. In layer 3 a normalization process will be done using equation 1.

$$\bar{w}_1 = \frac{w_1}{w_1 + w_2} \tag{1}$$

The output of each node in layer 4 is computed using $o_i = \bar{w}_i \times Z_i = \bar{w}_i \times (p_i x_1 + q_i x_2 + r_i)$. The $\bar{w}_i$ variable is the output of layes 3 nodes and $\{p_i, q_i, r_i\}$ are the parameter set which should be computed in learning phase of the ANFIS structure. Output of the ANFIS structure is computed using the equation 2 as follows.

$$out = f(x_1, x_2) = \sum_i \bar{w}_i \times f_i \tag{2}$$

The unknown parameters of the ANFIS algorithm can be computed using any suitable optimization algorithm like gradient decent, genetic algorithm and etc.

RBF algorithm

At first Broomhead et. al. proposed the RBF network as a soft-computing algorithm which is used successfuly in many engineering applications such as function approximation, data classification, system control and etc.[22-25].

Three main layers, input, hidden and output layer constitute the RBF structure as shown in Fig. 2. The values of the input varibles (systems inputs) are delivered to the multi-variate Gaussian activation functions in hidden layer using the input neurons in layer 1. A weighted sum approach is used to compute the overall output of the system in the output layer. It is worth to note that the RBF algorithm is used for modelling a multi-inputs and single output system.

An instatiation of a RBF network for two inputs and one output system is shown in Fig. 2 with two input neurons, 4 Gaussian hidden neurons and one linear output neuron. Equation 3 shows the activation function of the Gaussian neuron in hidden layer. In this equation, the y_j is the output of the *j*th hidden neuron, $\vec{x}$ is the input vector which is defined as $\vec{x} = [x_1, x_2]$, $\vec{\mu}_j$ is the center of *j*th

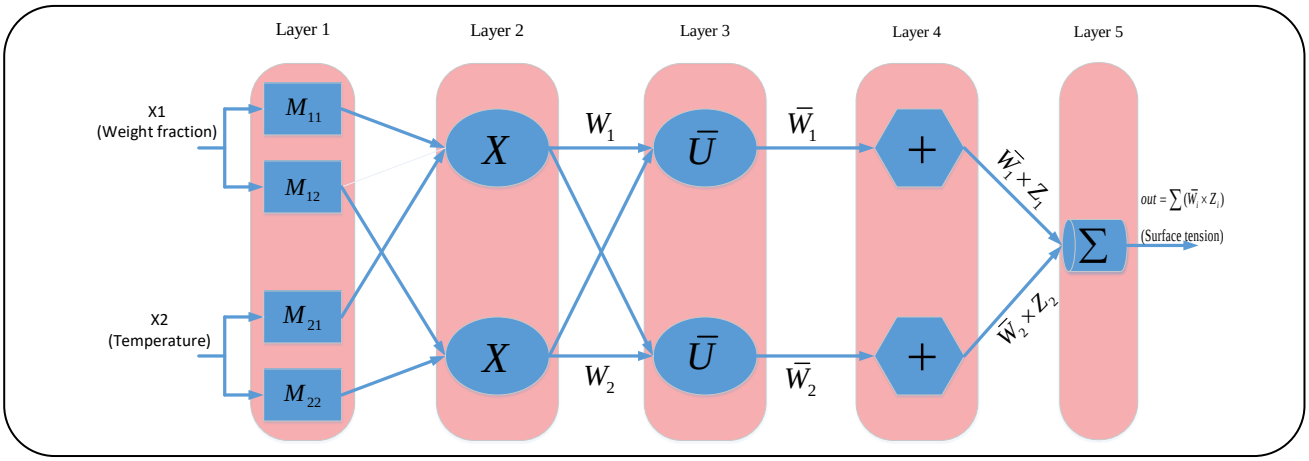

Fig. 1: Structure of ANFIS algorithm.

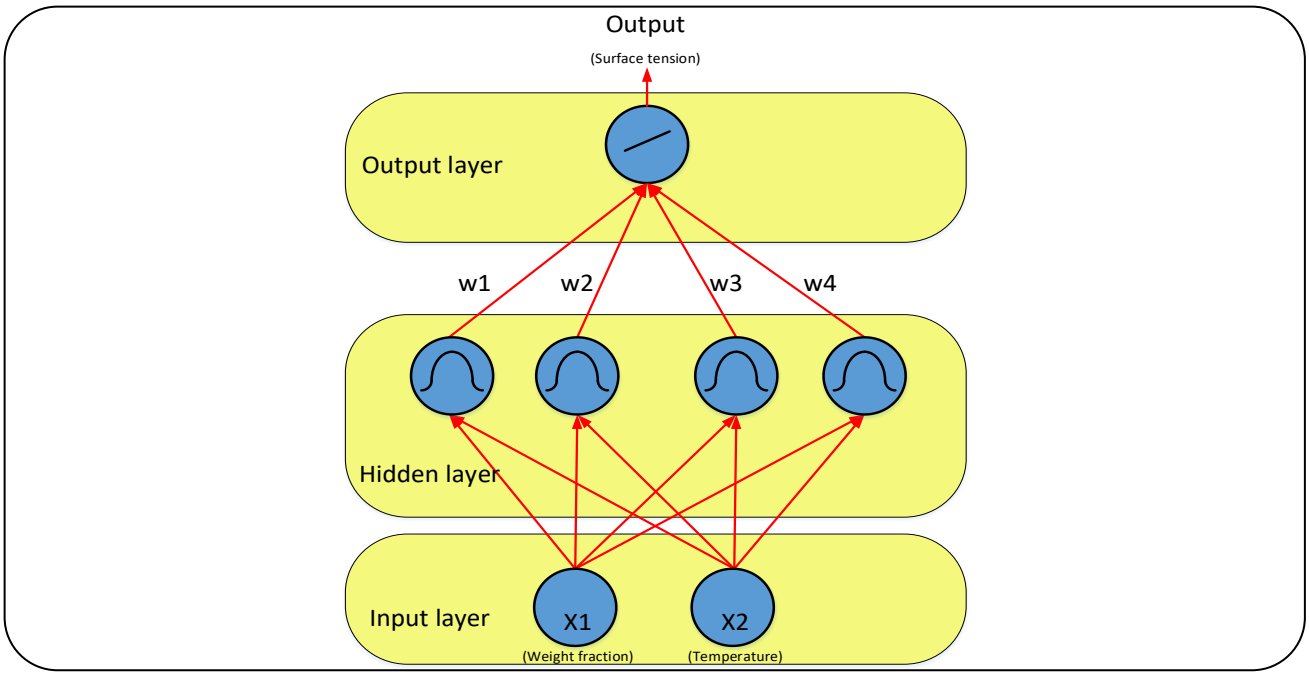

Fig. 1 RBF structure for a two inputs and one output system.

hidden neuron which is defined by $\vec{\mu}_j = [\mu_{1j}, \mu_{2j}]$ and σ_j is the variance of the Gaussian function and assumed equal for both x_1 and x_2 variables.

$$y_j = \exp\left(\frac{-\| \vec{x} - \vec{\mu}_j \|^2}{\sigma_j^2}\right) \quad (3)$$

Output of the system is computed using Eq. (4) using a linear combination of the hidden neurons output.

$$y\_out = \sum_j w_j y_j = \sum_j w_j \exp\left(\frac{-\| \vec{x} - \vec{\mu}_j \|^2}{\sigma_j^2}\right) \quad (4)$$

Training the RBF network can be done by minimization of the error term which is defined in eq. (5) using a suitable optimization algorithm [26-27]. In this equation, y_{ti} is the real output of the ith training sample and y_{mi} is the output of the constructed model.

$$\text{Error} = \sum_{i=1}^{n} \| y_{ti} - y_{mi} \|^2 \quad (5)$$

MLP algorithm

Artificial neural network algorithms was inspired form the human biological brain system[28]. MLP

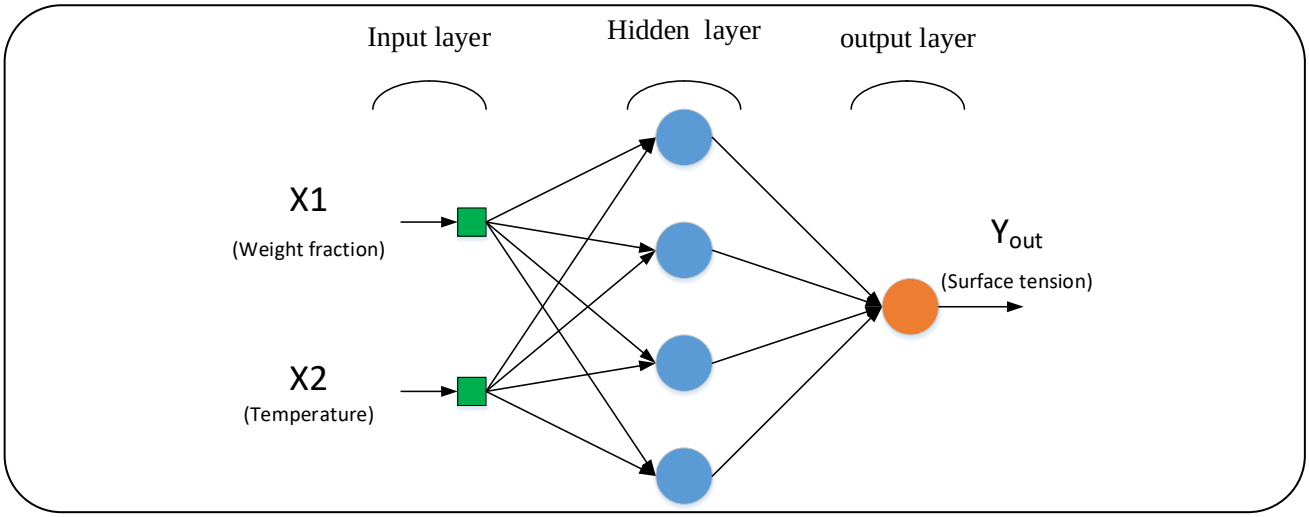

Fig. 2: Structure of 3 layers MLP model.

is a well-known algorithm in this area for solving complicated nonlinear problem [29-32]. MLP consists of at least three layers (input, hidden and output) in a feed-forward structure. Input neurons in the first layer delivers the value of the input variables of the system to the next layer through the synaptic weights. Hidden layers consist of perceptron neurons as a basic processing elements which sums its input and apply a nonlinear function (usually sigmoid) to the summation result. Using the nonlinear neurons, hidden layer increases the nonlinear modelling ability of the network for solving complex problems. In Fig. 3 a sample structure of a MLP network with two inputs and one output is shown.

Synaptic weights of the network are the parameter of the structure which should be defined using a suitable algorithm in the training phase. Back propagation which is proposed in [33] is a well-known and significant training algorithm of MLP, is using in many applications.

AGIDS algorithm

Also Active Learning Method(ALM) performs very well as fuzzy modeling algorithm in many engineering applications such as pattern classification, system modeling, control and etc., but because of hardware implementation complexity and need of time consuming optimization algorithms, its not suitable for many real-time real-world applications [34-38]. Trying to solve the ALMs defficacies resulted in proposition of the AGIDS algorithms by Esmaili et. al. in [39]. AGIDS is one of the last researches which has been done for solving these drawbacks in recent years[40-42]. Modeling a complex MISO (Multi-Inputs Single-output) system by breaking it to some simple SISO (Single-Input Single-Output) systems is the idea of ALM algorithm. Each SISO system is shown by an IDS plane which is an image with resolution rsn_x*rsn_y (rsn_x and rsn_y are number of quantization levels in x and y axis direction respectively) as an pictorial modeling technique. Each IDS plane is construted by mapping each training data (x,y) using IDS operator which is implemented by placing a pyramid shape stain on the IDS plane for each training data as a diffusion operator. In Fig.4-a, a pyramid shape ink stain is shown, also a sample IDS plane with five diffused data on it, is shown in Fig.4-b.

AGIDS uses the concept of the IDS plane and forms an IDS group for each training data which consists of *k* IDS planes for a system with *k* inputs and one output. The radius of the inks and the number of quantiztion level of the IDS plane are two parameters which can be defined by trial and error approach. In Fig. 5, a sample constructed model using AGIDS algorithm is shown for a two inputs one ouput system. The pictorial model can be shown by some proper *if then* rules too. The models output will be computed by applying two fuzzy operators, T-norm and S-norm, on the antecedent and consequent parts of the rules respectively. output of the model is fuzzy number which defines a confidence degree for each quantization level of the output variable. The fuzzy number can be converted to a crisp number by any suitable deffuzifier like Weighted Average Formula (WAF). AGIDS has been shown

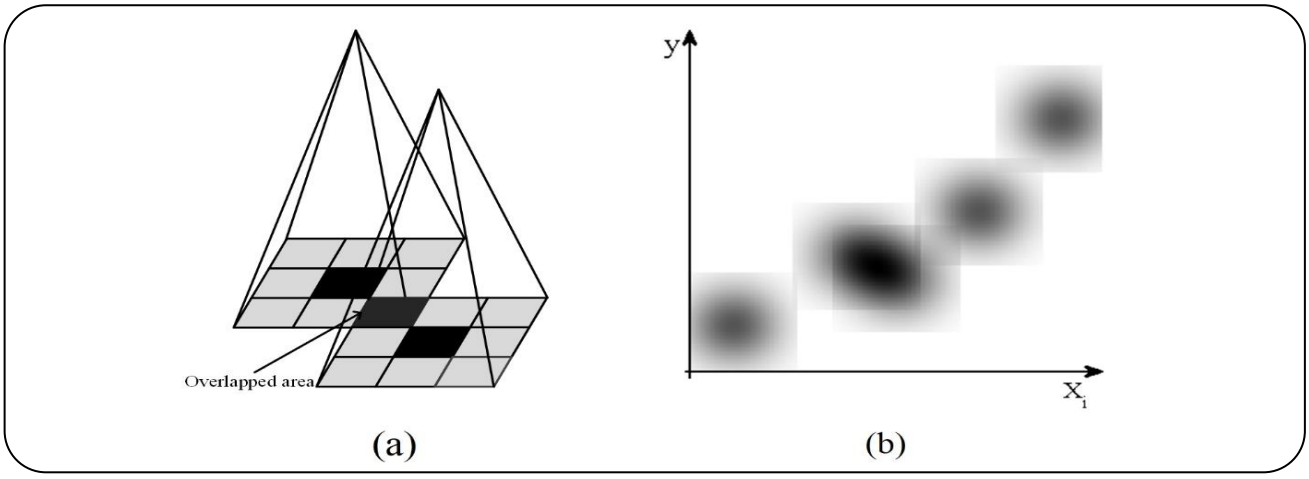

Fig. 3: a) Two Pyramid shape ink stains with overlap b)applying IDS operator for five sample data on an IDS plane [36].

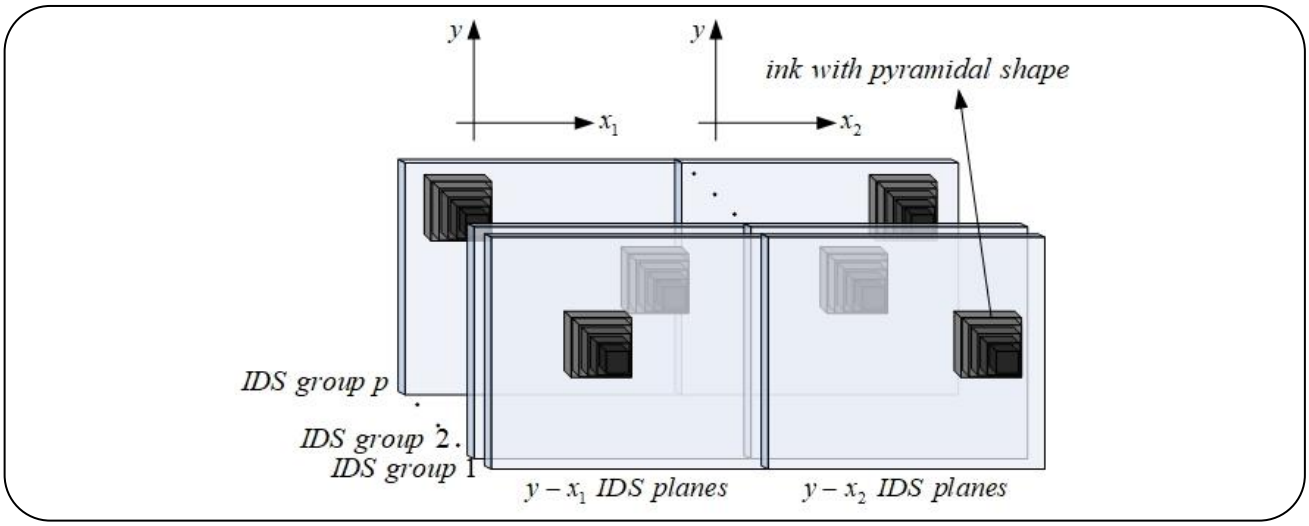

Fig. 4: IDS groups for a two-inputs and one output system with p sample data [36].

its effectiveness in different applications vs. other conventional algorithms [36,40].

RESULTS AND DISCUSSION

The experimental data of surface tensions of different polymer solutions are presented in Tables 1-4.

In this section, using the experimental data, the simulation results of modeling of the surface tension using the four aforementioned algorithms are explained. In this work, four aqueous polymer solutions(PEG 200 + Water, PEG 300 + Water, PEG 6000 + Water and PPG 2000 +Ethanol) were considered. According to data, surface tension is a function of weight fraction and temperature. As can been seen, when weight fraction of polymer increased, the surface tension decreased. In adtion when temperature of solution increased, the surface tension decreased.

Evaluation of modeling accuracy is done using two well-known measurement indexes in machine learning application, Fractional Variance Unexplained (FVU) and Mean Square Error (MSE) which are defined as Equations (6) and (7).

$$\mathrm{MSE} = \frac{1}{n}\sum_{i=1}^{n}(y_i - \hat{y}_i) \tag{6}$$

$$\mathrm{FVU} = \frac{\sum_{i=1}^{n}(y_i - \hat{y}_i)^2}{\sum_{i=1}^{n}(y_i - \bar{y})^2} \tag{6}$$

Table 1: Measured surface tension of PEG 200 + Water solutions at various temperatures/K and concentrations.

	T/K =303.15		T/K =308.15
w	$\sigma_{exp.}$ / (mN/m)	w	$\sigma_{exp.}$ / (mN/m)
0.1493	59.85	0.1493	58.81
0.222	57.88	0.222	56.85
0.2329	57.68	0.2329	56.64
0.3828	54.63	0.3828	53.58
0.4481	52.79	0.4481	51.75
0.467	52.05	0.467	51.08
0.5197	51.49	0.5197	50.46
0.5586	50.63	0.5586	49.62
0.6411	49.39	0.6411	48.28
0.712	47.58	0.712	46.54
0.7328	47.26	0.7328	46.22
	T/K =313.15		T/K =318.15
w	$\sigma_{exp.}$ / (mN/m)	w	$\sigma_{exp.}$ / (mN/m)
0.1493	57.87	0.1493	56.83
0.222	55.81	0.222	54.99
0.2329	55.59	0.2329	54.55
0.3828	52.65	0.3828	51.71
0.4481	50.82	0.4481	49.81
0.467	50.19	0.467	49.39
0.5197	49.45	0.5197	48.55
0.5586	48.72	0.5586	48.12
0.6411	47.12	0.6411	46.17
0.712	45.51	0.712	44.69
0.7328	45.19	0.7328	44.28
	T/K =323.15		T/K =328.15
w	$\sigma_{exp.}$ / (mN/m)	w	$\sigma_{exp.}$ / (mN/m)
0.1493	55.77	0.1493	54.66
0.222	54.07	0.222	53.3
0.2329	53.5	0.2329	52.56
0.3828	50.99	0.3828	50.36
0.4481	49.21	0.4481	48.19
0.467	48.49	0.467	47.43
0.5197	47.52	0.5197	46.44
0.5586	46.84	0.5586	45.49
0.6411	45.25	0.6411	44.23
0.712	43.98	0.712	43.17
0.7328	43.57	0.7328	43.06
	T/K =333.15		T/K =338.15
w	$\sigma_{exp.}$ / (mN/m)	w	$\sigma_{exp.}$ / (mN/m)
0.1493	53.66	0.1493	52.73
0.222	52.57	0.222	51.63
0.2329	51.42	0.2329	50.49
0.3828	49.25	0.3828	48.23
0.4481	46.93	0.4481	45.99
0.467	46.26	0.467	45.34
0.5197	45.41	0.5197	44.39
0.5586	44.48	0.5586	43.25
0.6411	43.09	0.6411	42.51
0.712	42.35	0.712	41.61
0.7328	42.65	0.7328	41.93

Table 2: Measured surface tension of PEG 300 + Water solutions at various temperatures/K and concentrations.

	T/K =298.15		T/K =303.15
w	$\sigma_{exp.}$ / (mN/m)	w	$\sigma_{exp.}$ / (mN/m)
0.108	60.03	0.108	59.09
0.1998	57.69	0.1998	56.66
0.2987	53.6	0.2987	52.67
0.3926	51.98	0.3926	50.92
	T/K =308.15		T/K =313.15
w	$\sigma_{exp.}$ / (mN/m)	w	$\sigma_{exp.}$ / (mN/m)
0.108	58.16	0.108	57.44
0.1998	55.71	0.1998	54.58
0.2987	52.27	0.2987	51.54
0.3926	49.92	0.3926	48.41
	T/K =318.15		T/K =323.15
w	$\sigma_{exp.}$ / (mN/m)	w	$\sigma_{exp.}$ / (mN/m)
0.108	56.73	0.108	55.46
0.1998	53.3	0.1998	52.42
0.2987	50.52	0.2987	49.51
0.3926	47.89	0.3926	46.81
	T/K =328.15		T/K =333.15
w	$\sigma_{exp.}$ / (mN/m)	w	$\sigma_{exp.}$ / (mN/m)
0.108	54.73	0.108	53.58
0.1998	51.44	0.1998	50.37
0.2987	48.38	0.2987	47.21
0.3926	46.29	0.3926	45.27
	T/K =338.15		
w	$\sigma_{exp.}$ / (mN/m)		
0.108	52.58		
0.1998	48.57		
0.2987	46.35		
0.3926	44.19		

Table 3: Measured surface tension of PEG 6000 + Water solutions at various temperatures/K and concentrations.

	T/K =298.15		T/K =303.15
w	$\sigma_{exp.}$ / (mN/m)	w	$\sigma_{exp.}$ / (mN/m)
0.0399	59.87	0.0399	58.84
0. 0601	59.02	0. 0601	58.4
0.0982	58.26	0.0982	57.23
0.1974	57.13	0.1974	56.11
	T/K =308.15		T/K =313.15
w	$\sigma_{exp.}$ / (mN/m)	w	$\sigma_{exp.}$ / (mN/m)
0.0399	57.98	0.0399	57.25
0. 0601	57.4	0. 0601	56.37
0.0982	56.71	0.0982	55.79
0.1974	54.84	0.1974	53.69
	T/K =318.15		T/K =323.15
w	$\sigma_{exp.}$ / (mN/m)	w	$\sigma_{exp.}$ / (mN/m)
0.0399	55.74	0.0399	54.69
0. 0601	55.35	0. 0601	54.29
0.0982	54.73	0.0982	53.37
0.1974	52.65	0.1974	51.62
	T/K =328.15		T/K =333.15
w	$\sigma_{exp.}$ / (mN/m)	w	$\sigma_{exp.}$ / (mN/m)
0.0399	53.64	0.0399	52.61
0. 0601	53.83	0. 0601	52.22
0.0982	52.23	0.0982	51.19
0.1974	50.59	0.1974	49.47
	T/K =338.15		
w	$\sigma_{exp.}$ / (mN/m)		
0.0399	51.27		
0. 0601	51.42		
0.0982	50.17		
0.1974	48.28		

Table 4: Measured surface tension of PPG 2000 + Ethanol solutions at various temperatures/K and concentrations.

	T/K =298.15		T/K =303.15
w	$\sigma_{exp.}$ / (mN/m)	w	$\sigma_{exp.}$ / (mN/m)
0.1	22.14	0.1	21.54
0.2	22.44	0.2	21.84
0.3	22.64	0.3	22.14
0.4	22.94	0.4	22.44
	T/K =308.15		T/K =313.15
w	$\sigma_{exp.}$ / (mN/m)	w	$\sigma_{exp.}$ / (mN/m)
0.1	21.24	0.1	20.54
0.2	21.34	0.2	20.84
0.3	21.64	0.3	21.34
0.4	22.24	0.4	21.94
	T/K =318.15		T/K =323.15
w	$\sigma_{exp.}$ / (mN/m)	w	$\sigma_{exp.}$ / (mN/m)
0.1	20.34	0.1	19.84
0.2	20.44	0.2	20.13
0.3	20.84	0.3	20.44
0.4	21.44	0.4	21.24
	T/K =328.15		T/K =333.15
w	$\sigma_{exp.}$ / (mN/m)	w	$\sigma_{exp.}$ / (mN/m)
0.1	19.44	0.1	19.26
0.2	19.63	0.2	19.32
0.3	20.34	0.3	20.03
0.4	21.54	0.4	20.68
	T/K =338.15		
w	$\sigma_{exp.}$ / (mN/m)		
0.1	18.78		
0.2	18.92		
0.3	19.42		
0.4	20.29		

Where *n* is the number of test data, y_i is the real output, $\hat{y}_i$ is the model's output and $\bar{y}$ is the mean value of the real outputs which is defined with $\bar{y} = \frac{1}{n}\sum_{i=1}^{n}(y_i)$. The FVU is a normalized index which by increasing the model accuracy it will decrease to zero.

The number of quantization levels and the ink radius for AGIDS algorithm are set to 64 and 4 respectively. The number of neurons in hidden layer of MLP algorithm is set to 10 and the activation function are *tansig* for hidden layer and linear for output layer. For the purpose of simulations, 70 percent of the data are used as training set

Table 5: Comparison of four algorithm performance in modeling task .

]	algorithm	FVU(mean)	FVU(std)	MSE(mean)	MSE(std)
PEG 200 + Water solutions	AGIDS	0.0466	0.0123	0.8524	0.1601
	MLP	0.0112	0.0082	0.4364	0.1030
	RBF	0.0046	0.0008	0.3272	0.0270
	ANFIS	0.0083	0.0023	0.0324	0.2545
PEG 300 + Water solutions	AGIDS	0.0595	0.0170	0.8488	0.1069
	MLP	0.0196	0.0112	0.5042	0.1380
	RBF	0.0116	0.0028	0.4059	0.0347
	ANFIS	0.0111	0.0034	0.0304	0.2737
PEG 6000 + Water solutions	AGIDS	0.1286	0.0434	0.9007	0.2907
	MLP	0.0323	0.0232	0.5147	0.3313
	RBF	0.0073	0.0025	0.2236	0.0159
	ANFIS	0.0082	0.0023	0.0055	0.1152
PPG 2000 + Ethanol solutions	AGIDS	0.2441	0.0625	0.4634	0.0521
	MLP	0.1300	0.0643	0.3507	0.0928
	RBF	0.0190	0.0196	0.1267	0.0133
	ANFIS	0.1089	0.0836	0.0106	0.2338

and the rest 30 percent are used for test. All data are being normalized using the Equation (8) to have zero mean and variation of one.

$$x_{normal} = \frac{x - \bar{x}}{\sigma} \tag{8}$$

Where x, $\bar{x}$ and σ are the actual, mean and variance values of observed data respectively.

In Table 5 the quantitative comparison of four algorithms performance is shown. Simulations are done for 100 times run and the mean and standard deviation of the results are reported. From the table, it can be deduced that ANFIS and RBF performance in modeling this phenomenon is better than respect to the other two algorithms. Both MSE and FVU indexes confirm this conclusion.

In Fig. 6, a qualitative comparison for PEG 200 + Water solutions is done. Actually, the 3D surfaces of the four models are shown in the Fig. 6-a to Fig. 6-d. Each figure shows the surface tension vs. temperature and weight fraction. As can be seen from these figures, the result of ANFIS and RBF algorithms are similar together as a hyper plane surface vs the other two which have more non-linearity in the shape. A similar qualitative comparison is done for PEG 300 + Water solutions, PPG 2000 + Ethanol solutions and PPG 2000 + Ethanol solutions which is shown in Figs. 7 to 9 with similar results.

The regression coefficients for these four algorithms are being computed for more convenience and as can be conducted from Figs. 10 to 13, the regression coefficients confirm the results of Table 1 and Figs. 6 to 9.

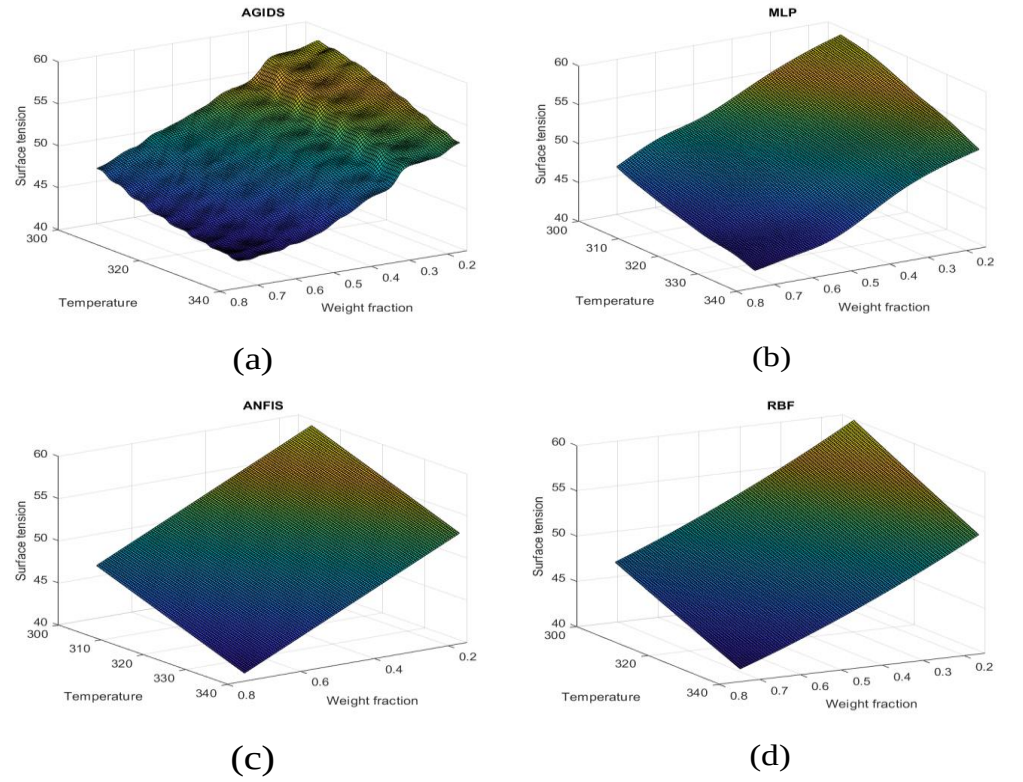

Fig. 5: The modeling surface for a) AGIDS, b) MLP, c)ANFIS and d)RBF algorithms(PEG 200 + Water solutions).

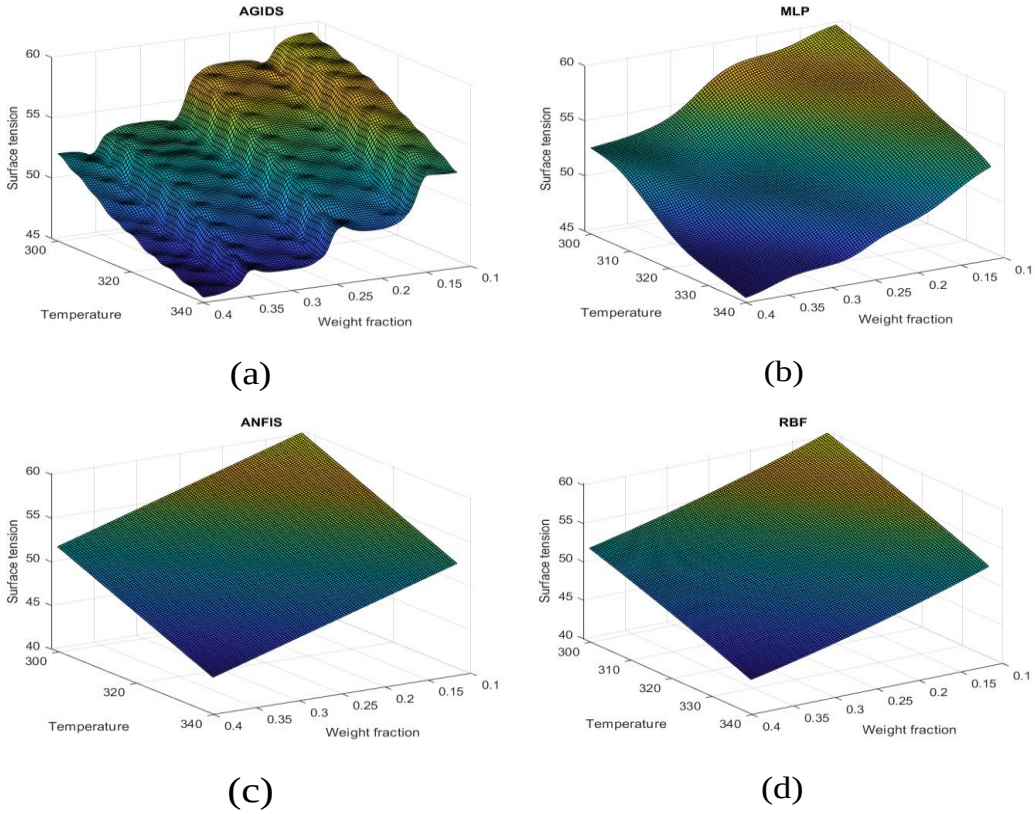

Fig. 7: The modeling surface for a) AGIDS, b) MLP, c) ANFIS and d)RBF algorithms(PEG 300 + Water solutions).

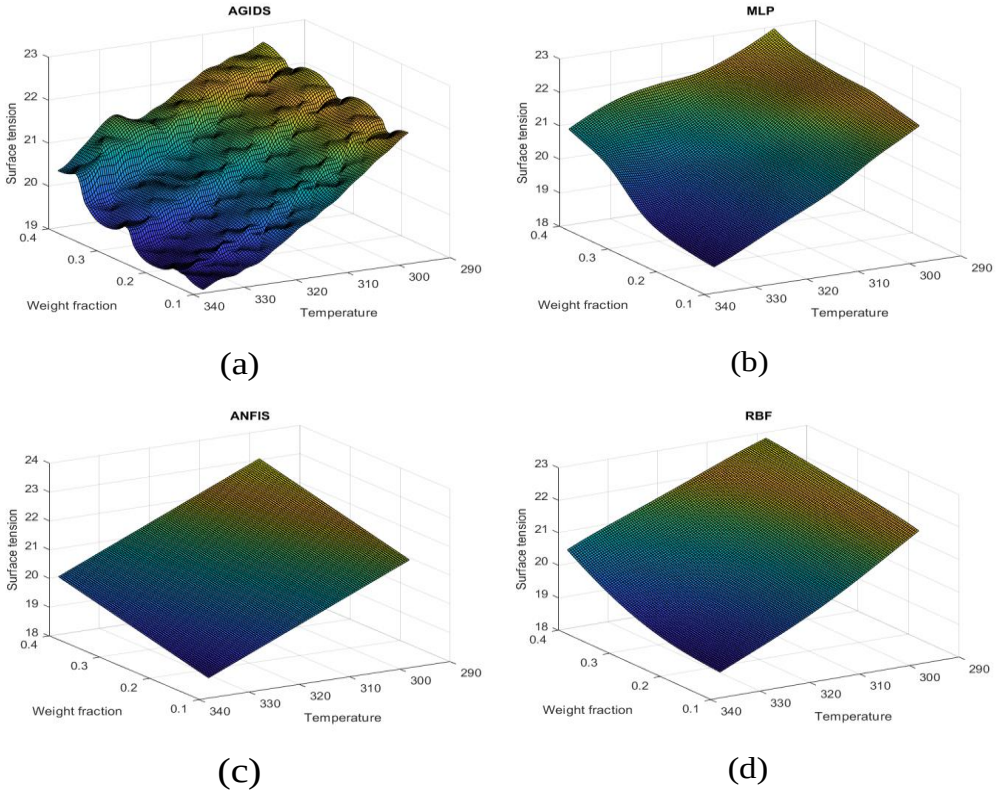

Fig. 8: The modeling surface for a) AGIDS, b) MLP, c)ANFIS and d)RBF algorithms(PPG 2000 + Water solutions).

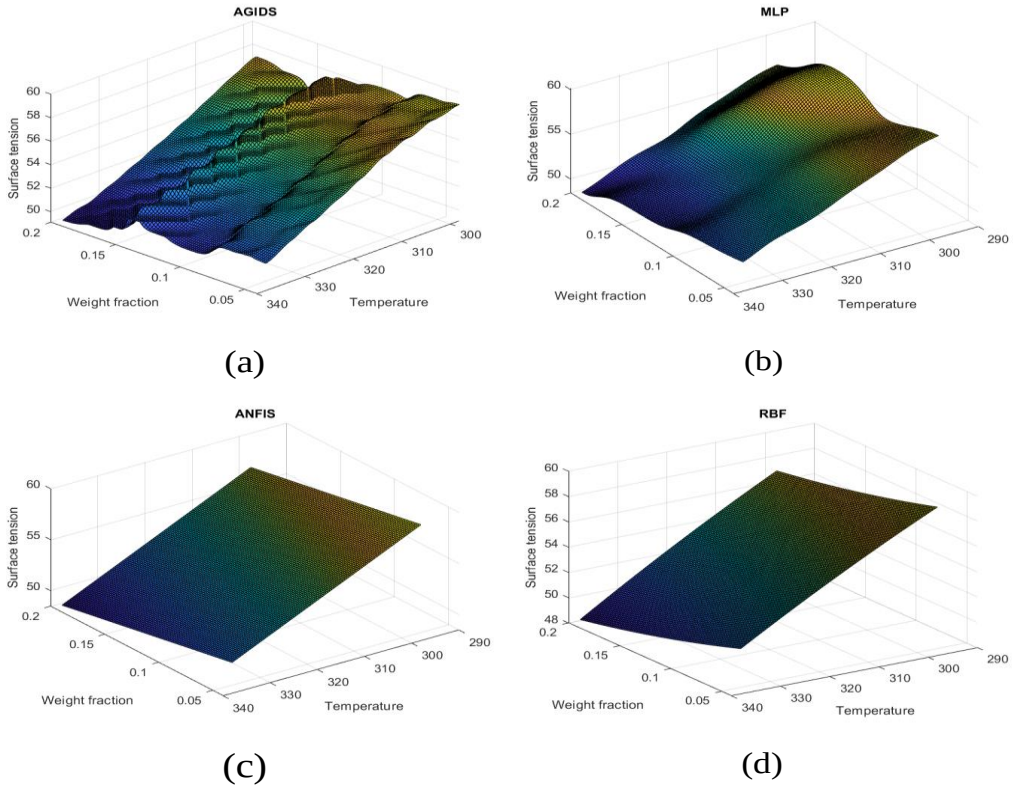

Fig. 9: The modeling surface for a) AGIDS, b) MLP, c)ANFIS and d)RBF algorithms(PEG 6000 + Water solutions).

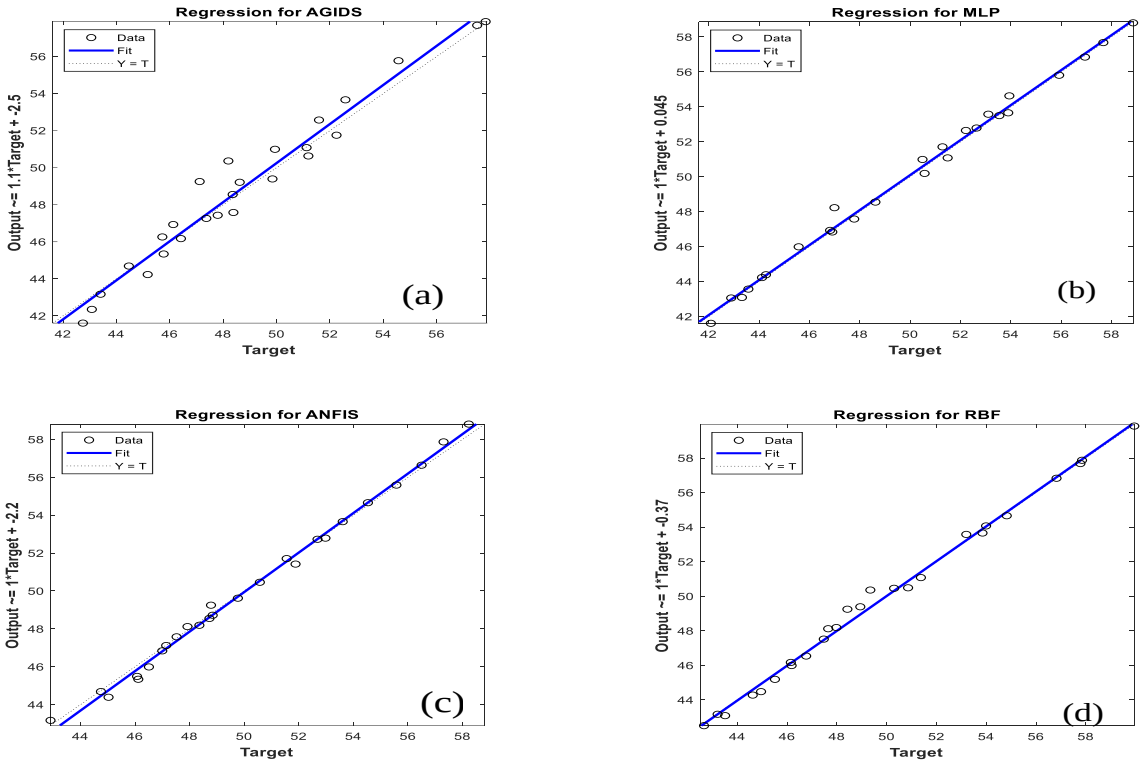

Fig. 10: The regression coefficient for a) AGIDS(0.9835), b) MLP(0.9964), c) ANFIS(0.9965) d) RBF(0.9978) algorithms (PEG 200 + Water solutions).

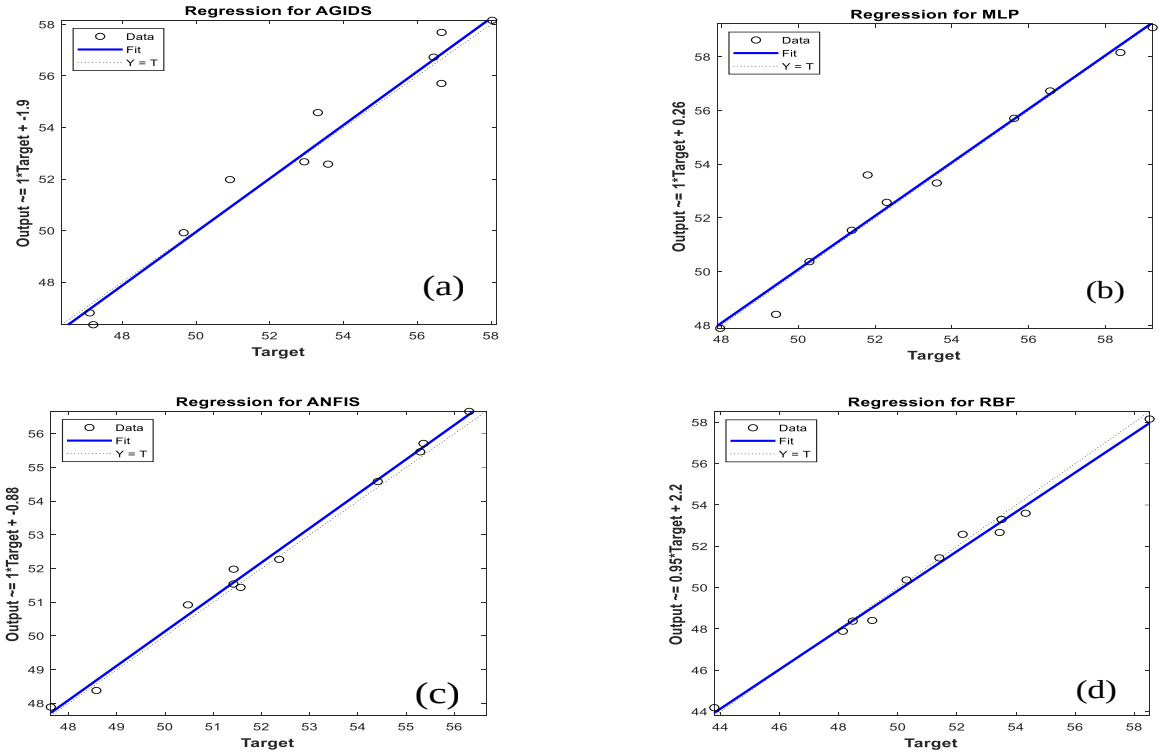

Fig. 11: The regression coefficient for a) AGIDS(0.9755), b) MLP(0.9964), c) ANFIS(0.9963) d) RBF(0.9954) algorithms (PEG 300 + Water solutions).

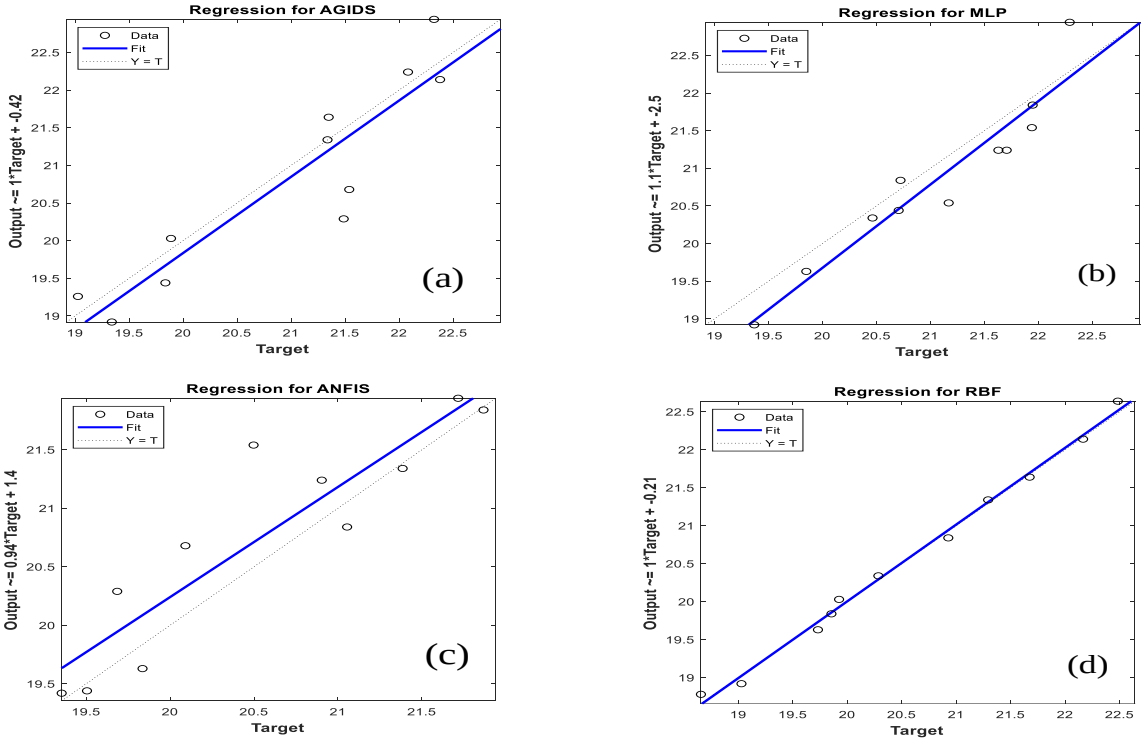

Fig. 12: The regression coefficient for a) AGIDS(0.9311), b) MLP(0.9577), c) ANFIS(0.9585) d) RBF(0.9916) algorithms(PPG 2000 + Water solutions).

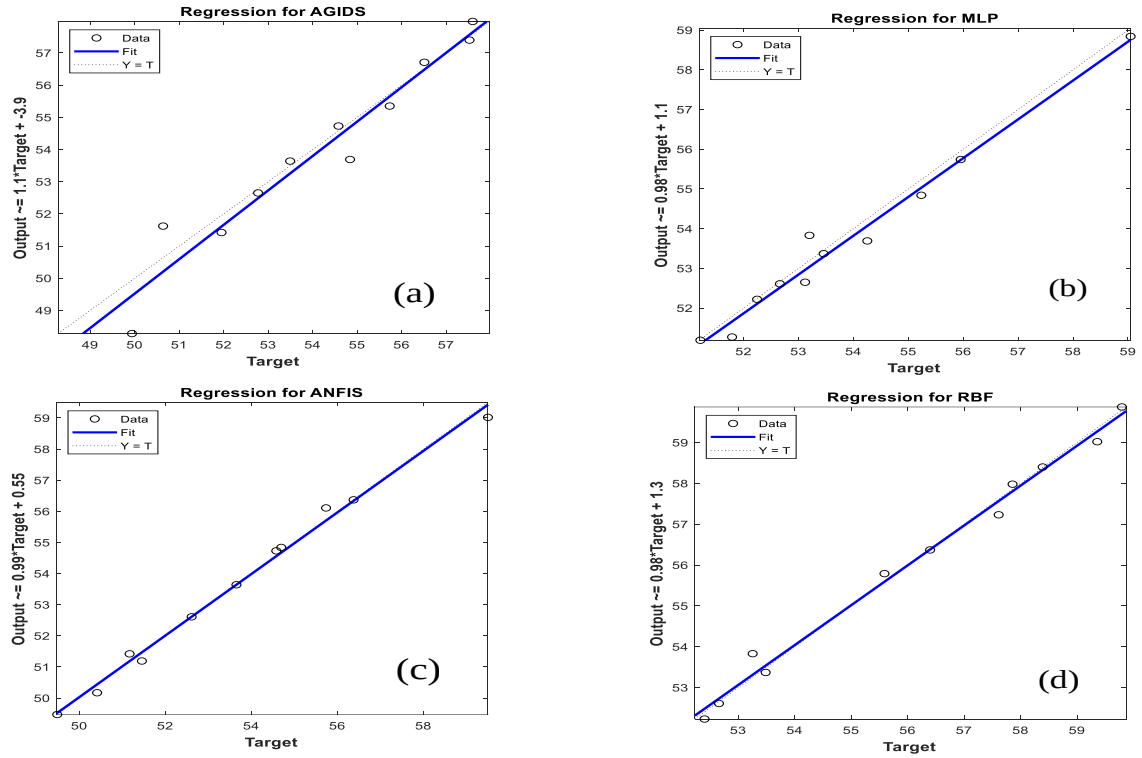

Fig. 13: The regression coefficient for a) AGIDS(0.9588), b) MLP(0.9896), c) ANFIS(0.9964) d) RBF(0.9968) algorithms(PEG 6000 + Water solutions).

CONCLUSIONS

In this study, the ability of AGIDS (fuzzy approach), MLP, RBF (both from neural network approach) and ANFIS (neuro-fuzzy approach) algorithms were examined for their effectiveness to represent a wide surface tension on the aqueous polymer over a wide range of temperature and composition. The prediction results from simulations, was in a good agreement with experimental data. It can be concluded from the simulation results that the application of soft-computing models can be considered as an alternative for description of surface tension of aqueous polymer behavior and their responses are in a good agreement with experimental data. Based on the simulation results, ANFIS and RBF models performs the modeling task better than the other two algorithms in this problem. It should be noted that the effectiveness of these algorithms will be better with more existed experimental data. Using soft computing algorithms can be an effective approach in prediction of the chemical systems behavior, so it can reduce the experimental approaches costs.

Received May 8, 2022 : ; Accepted : Sep. 26,2022

REFERENCES

[1] Hu R.Y.Z., Wang A.T.A., Hartnett J.P., Surface Tension Measurement of Aqueous Polymer Solutions, *Experimental Thermal and Fluid Science*, **4(6)**: 723-729 (1991).

[2] Wu S., Interfacial and Surface Tensions of Polymers, *Journal of Macromolecular Science—Reviews in Macromolecular Chemistry*, **10(1)**: 1-73 (1974).

[3] Szymczyk K, Zdziennicka A., Wettability, Adhesion, Adsorption and Interface Tension in the Polymer/Surfactant Aqueous Solution System. I. Critical surface tension of polymer wetting and its surface tension, *Colloids and Surfaces A: Physicochemical and Engineering Aspects*, **402**: 132–138 (2012).

[4] Sharma S., Kamil M., Studies on the Interaction Between Polymer and Surfactant in Aqueous Solutions, *Ind. J. of Chemical Technol.*, **25(3)**: 294-299 (2018)

[5] Vis M., Blokhuis E.M., Interfacial Tension of Phase-Separated Polydisperse Mixed Polymer Solutions, *J. Phys. Chem. B*, **122**: 3354−3362 (2018).

[6] Nath S., Surface Tension of Nonideal Binary Liquid Mixtures as a Function of Composition, *Journal of Colloid and Interface Science*, **209(1)**: 116-122 (1999).

[7] Larsen B.L., Rasmussen P., Fredenslund A., A Modified UNIFAC Group-Contribution Model for Prediction of Phase Equilibria and Heats of Mixing, *Industrial & Engineering Chemistry Research*, **26(11)**: 2274-2286 (1987).

[8] Bongiorno V., Davis H.T., Modified Van Der Waals Theory of Fluid Interfaces, *Physical Review* A, **12(5)**: 2213 (1975).

[9] Babuška R., Verbruggen H.B., An Overview of Fuzzy Modeling for Control, *Control Engineering Practice*, **4(11)**: 1593-1606 (1996).

[10] Roy D.G., Singh T.N., Regression and Soft-Computing Models to Estimate Young's Modulus of CO2 Saturated Coals, *Measurement*, **129**: 91-101 (2018).

[11] Vaidyanathan S., Zhu Q., Azar A.T., Adaptive Control of a Novel Nonlinear Double Convection Chaotic System, In: "Fractional Order Control and Synchronization of Chaotic Systems" (pp. 357-385). Springer, Cham (2017).

[12] Singh R., Umrao R.K., Ahmad M., Ansari M.K., Sharma L.K., Singh T.N., Prediction of Geomechanical Parameters Using Soft-Computing and Multiple Regression Approach, *Measurement*, **99**: 108-119 (2017).

[13] Liu Y., Zhang Y., Iterative Local ANFIS-Based Human Welder Intelligence Modeling and Control in Pipe GTAW Process: A Data-Driven Approach, *IEEE/ASME Transactions on Mechatronics*, **20(3)**: 1079-1088 (2014).

[14] Wu Q., Wang, X., Shen Q., Research on Dynamic Modeling and Simulation of Axial-Flow Pumping System Based on RBF Neural Network, *Neurocomputing*, **186**: 200-206 (2016).

[15] Amooey A.A., Fazlollahnejad M., Study of Surface Tension of Binary Mixtures of Poly (Ethylene Glycol) in Water and Poly (Propylene Glycol) in Ethanol and its Modeling Using Neural Network (2014).

[16] Vakili M., Yahyaei M., Kalhor K., Thermal Conductivity Modeling of Graphene Nanoplatelets/Deionized Water Nanofluid by MLP Neural Network and Theoretical Modeling Using Experimental Results, *International Communications in Heat and Mass Transfer*, **74**: 11-17 (2016).

[17] Jang J.S., ANFIS: Adaptive-Network-based Fuzzy Inference System, *IEEE Transactions on Systems, man, and cybernetics*, **23(3)**: 665-685 (1993).

[18] Hosoz,M., et al., ANFIS Modelling of the Performance and Emissions of a Diesel Engine Using Diesel Fuel and Biodiesel Blends, *Applied Thermal Engineering*, **60(1-2)**: 24-32 (2013).

[19] Fu Y., Yang H., Ding J., Multiple Operating Mode ANFIS Modelling for Speed Control of HSEMU, *IET Intelligent Transport Systems*, **12(1)**: 31-40 (2017).

[20] Veluchamy B., Karthikeyan N., Krishnan B.R., Sundaram C.M., Surface Roughness Accuracy Prediction in Turning of Al7075 by Adaptive Neuro-Fuzzy Inference System, *Materials Today: Proceedings*, **37**: 1356-1358 (2021).

[21] Raj A.S., Oliver D.H., Srinivas Y., Geoelectrical Data Processing Using Neuro Fuzzy Pattern Recognition Scheme for Unambiguous Subsurface Modelling. *International Journal of Hydrology Science and Technology*, **7(4)**: 364-389 (2017).

[22] Broomhead D.S., Lowe D., "Radial Basis Functions, Multi-Variable Functional Interpolation and Adaptive Networks", Royal Signals and Radar Establishment Malvern (United Kingdom) (1988).

[23] Lazzaro D., Montefusco L.B., Radial Basis Functions for the Multivariate Interpolation of Large Scattered Data sets, *Journal of Computational and Applied Mathematics*, **140(1-2)**: 521-536 (2002).

[24] Belloir F., Fache A., Billat A., April. A General Approach to Construct RBF Net-Based Classifier, In "ESANN" (pp. 399-404) (1999).

[25] Li Y., et al., Robust and Adaptive Back Stepping Control for Nonlinear Systems Using RBF Neural Networks, *IEEE Transactions on Neural Networks*, **15(3)**: 693-701 (2004).

[26] Karayiannis N.B., "Gradient Descent Learning of Radial Basis Neural Networks", In: *Proceedings of International Conference on Neural Networks* (ICNN'97) (Vol. 3, pp. 1815-1820). IEEE (1997).

[27] Wu J., Long J., Liu M., Evolving RBF Neural Networks for Rainfall Prediction Using Hybrid Particle Swarm Optimization and Genetic Algorithm, *Neurocomputing*, **148**: 136-142 (2015).

[28] Ruck D.W., et al., The Multilayer Perceptron as an Approximation to a Bayes Optimal Discriminant Function, *IEEE Transactions on Neural Networks*, **1(4)**: 296-298 ( ).

[29] Norgaard M., Ravn O., Poulsen N.K., Hansen L.K., "Neural Networks for Modelling and Control of Dynamic Systems: A Practitioner's Handbook". London: Springer (2000).

[30] Gardner M.W., Dorling S., Artificial Neural Networks (the Multilayer Perceptron) a Review of Applications in the Atmospheric Sciences, *Atmospheric Environment*, **32(14-15)**: 2627-2636 (1998).

[31] Agirre-Basurko E., Ibarra-Berastegi G., Madariaga I., Regression and Multilayer Perceptron-Based Models to Forecast Hourly O_3 and NO_2 Levels in the Bilbao Area, *Environmental Modelling & Software*, **21(4)**: 430-446 (2006).

[32] Radha Krishnan B., Vijayan V., Parameshwaran Pillai T., Sathish T., Influence of Surface Roughness in Turning Process—An Analysis Using Artificial Neural Network, *Transactions of the Canadian Society for Mechanical Engineering*, **43(4)**: 509-514 (2019).

[33] Hecht-Nielsen R., Theory of the Backpropagation Neural Network. In Neural networks for perception (pp. 65-93). Academic Press (1992).

[34] Shouraki S.B., Recursive Fuzzy Modeling Based on Fuzzy Interpolation, *Journal of Advanced Computational Intelligence*, **3(2)**: 114-125 (1999).

[35] Murakami M., Honda N., A Study on the Modeling Ability of the IDS Method: A Soft Computing Technique Using Pattern-based Information Processing. *International Journal of Approximate Reasoning*, **45(3)**: 470-487 (2007).

[36] Firouzi M., Shouraki S.B., Afrakoti I.E.P., Pattern Analysis by Active Learning Method Classifier. *Journal of Intelligent & Fuzzy Systems*, **26(1)**: 49-62 (2014).

[37] Sagha H., Afrakoti I.E.P., Bagherishouraki S., Actor-Critic-Based Ink Drop Spread as an Intelligent Controller, *Turkish Journal of Electrical Engineering and Computer Sciences*, **21(4)**: 1015-1034 (2013).

[38] Afrakoti I.E.P., Shouraki S.B., Bayat F.M., Gholami M., Using a Memristor Crossbar Structure to Implement a Novel Adaptive Real-Time Fuzzy Modeling Algorithm, *Fuzzy Sets and Systems*, **307**: 115-128 (2017).

[39] Afrakoti I.E.P., Shouraki S.B., Haghighat B., An Optimal Hardware Implementation for Active Learning Method Based on Memristor Crossbar Structures, *IEEE Systems Journal*, **8(4)**: 1190-1199 (2014).

[40] Afrakoti I.E.P., Ghaffari A., Shouraki S.B., March. "Effective Partitioning of Input Domains for ALM Algorithm". In *2013 First Iranian Conference on Pattern Recognition and Image Analysis* (PRIA) (pp. 1-5). IEEE (2013).

[41] Sagha H., Shouraki S.B., Beigy H., Khasteh H., Enayati E., December. "Genetic Ink Drop Spread". In *2008 Second International Symposium on Intelligent Information Technology Application* (Vol. 2, pp. 603-607). IEEE (2008).

[42] Hosseini S.A., Afrakoti I.E.P., Adaptive Group of Ink Drop Spread: a Computer Code to Unfold Neutron Noise Sources in Reactor Cores, *Nuclear Engineering and Technology*, **49(7)**: 1369-1378 (2017).